Paper Number

A new test procedure to validate dynamic tensile mechanical properties of sheet metals and alloys in light weight automotive crash applications

P. K. C. Wood, C. A. Schley, G. F. Smith
IARC, University of Warwick, Coventry, England

M. Buckley
Jaguar and Land Rover

ABSTRACT

A thin walled open channel beam subjected to a 3-point bend and constant velocity boundary condition is investigated to establish its potential to validate material performance for automotive crash applications. Specifically quantitative validation of material data determined from high speed tensile testing and qualitative validation of material resistance to fracture in crash components. Open channel beams are fabricated from structural grade sheet steel and aluminium alloy and tested at quasi-static and higher speeds up to 10 m/s and in all cases, deformation develops a plastic hinge. This paper describes development of the validation test procedure, specifically design of specimen, system of measurement and boundary conditions using numerical and experimental techniques. The new test procedure will increase confidence in materials modelling and reduce the risk to introduce new advanced high strength materials into automotive crash structures.

INTRODUCTION

An improved understanding of the behaviour of automotive materials at high velocity is driven by the challenges of diverse crash legislation and competition amongst car manufacturers. In a round robin study involving ten leading international testing laboratories reported in 2006[1], uncertainty in material tensile data increases with strain rate, and particularly in the design range for automotive applications. The cost of generating material tensile data with strain rate dependency is high. A cost survey conducted as part of this study, and involving both academic and industry sources suggest a factor of typically fifty times higher than the cost to generate quasi-static tensile data to Euronorm[2] requirements.

The high cost and uncertainty in the quality of material strain rate sensitivity data is the motivation for this project. The aim of this study is to develop a bend-impact validation test as a compliment to crush testing components which by definition involves progressive self contact and more generally uses a two-part joined assembly (e.g. top hat to closure plate with multiple joints), which will increase complexity in material validation assessment. The bend-impact test considered is representative of some of the components and loadings in an automotive crash structure. This study will investigate the suitability of a thin-walled open channel beam, subject to a 3-point bend impact to validate material strain rate sensitivity data for use in developing lightweight premium automotive crash safety structures.

This study forms part of larger body of work, which considers the requirements for the generation of strain rate sensitivity data for ferrous and non-ferrous materials, together with the processes to transform, model, and to format this data for input to crash simulation tools, and finally to validate this data in representative crash structures. This project is supported by a luxury car-maker, a number of consulting and material suppliers to the premium automotive and other transport sectors.

EXPERIMENTAL INVESTIGATIONS

In the current test arrangement it was desirable to investigate a beam under simple 3-point bending rather than fix or constrain the ends of beam. Constraining the beam ends may be desirable to increase lateral stiffness and hence natural frequency. Uncertainty in the restraints (or end fixings) however, will create further uncertainty in measurements relating to material performance. There is concern that loading of beam at the four edge support contact points may induce an unpredictable beam collapse mode.

Experimental equipment

The equipment at the IARC is a high speed servo-hydraulic machine[3] with a stiff four column load frame capable of 160kN maximum dynamic loading. The actuator delivers constant velocity in the range 1 to 1000 mm/s under closed loop control, and 1000 through to 20000mm/s under open loop control. The transducer connecting impactor (tup) to the actuator is instrumented with a full bridge strain gauge circuit, see figure 1. Actuator movement is measured using a Linear Variable Differential Transducer (LVDT). Guides constrain tup movement to the loading axis, to minimise bending moment transfer to instrumented shaft, and suppress rotation of tup during loading cycle. Hydraulic oil is wiped along the inner slides of the guides to minimize friction resistance.

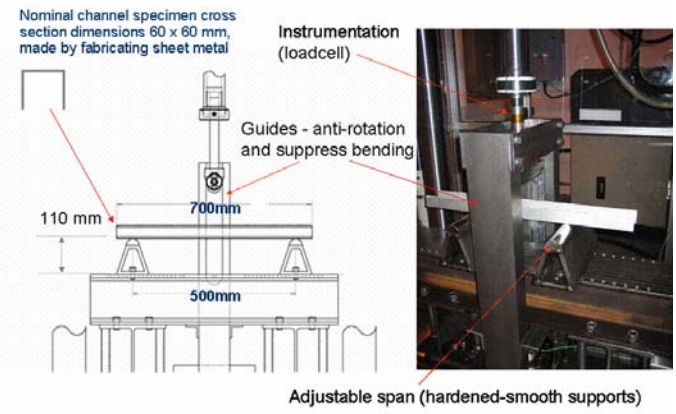

Figure 1: Bend-impact test arrangement: Specimen, fixture and boundary conditions

The actuator develops a full working stroke of 300 mm under open loop control which includes the distance required to accelerate actuator to constant velocity, and distance to decelerate actuator. The distance available for applied constant velocity during loading cycle decreases on demand for higher constant velocity. A further safety measure is the incorporation of shear pin connecting tup shaft to actuator, so designed to protect equipment should the inertia force exceed 60kN. Two hardened steel supports are designed to provide an adjustment to beam span depending on test requirements.

Specimen design

The nominal outer dimensions of beam specimen are 60 mm wide x 60 mm deep x 700 mm long. The nominal corner radius for the Dual Phase steel specimen is 3.5 mm to mid-plane of section, which is typical of a 1.5 mm gauge automotive steel pressing. The nominal corner radius of for the AA5754 aluminium alloy specimen is 8.75 mm to mid-plane of section for 2.5 mm gauge. Specimens are fabricated using a CNC folding machine with spring back compensation, to produce U-section specimens from sheet to a consistent high accuracy.

Experimental setup

The beam span between supports is maximised at 500 mm, to promote tensile (or direct) stress in side walls of beam rather than shear deformation.

To delay initiation of plastic hinge and hence premature bending collapse a large tup radius seems to be desirable to maximise contact area between tup and top surface of beam. But tup size is restricted to a smaller dimension to limit inertia force during deceleration phase of actuator. Preliminary CAE suggested dynamic loading would not exceed 30kN at high speed.

The current set up is designed to deliver a constant velocity over at least 50 mm from tup initial contact with beam. A limit of 50 mm range is necessary because at 20,000 mm/s the actuator requires a minimum 55 mm working stroke for deceleration. A larger displacement range could be used but requires a modification to fixture arrangement.

TEST MEASUREMENT ANALYSIS

Tests were conducted at five velocities to obtain quantitative measurements; these are 10, 100, 800, 2,000 and 5,000 mm/s. The measured velocity profiles are shown in the graph in upper figure 2. It is noted that deviation from target velocity value appears to increase with speed. The deviation between target and measured value for a given velocity is shown in lower figure 2. At lower velocity the average relative deviation is below 3% and is positive meaning the measured velocity is greater than target value. At higher velocity, the relative deviation rises to near 7% at 2,000 mm/s and is negative, meaning the measured velocity is smaller than target value.

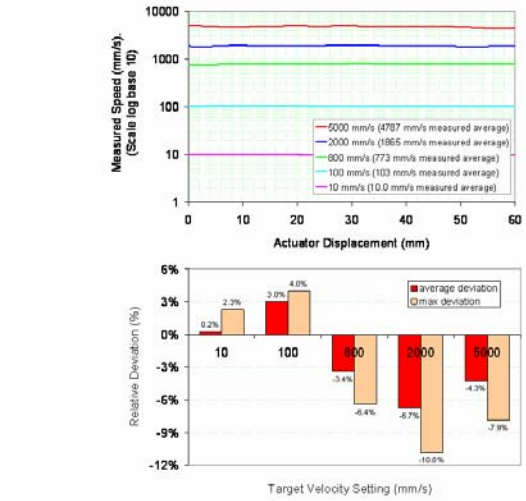

Figure 2: Measured velocities (upper). Measured velocity deviation from target (lower)

The machine control ‘velocity profile correction’ may be applied under open loop control which would reduce the error between target and measured velocity, but increasing overall complexity and set up time of test.

The target velocity values will be used however as boundary condition inputs to finite element models. For convenience the target values are referred to as nominal values from hereon.

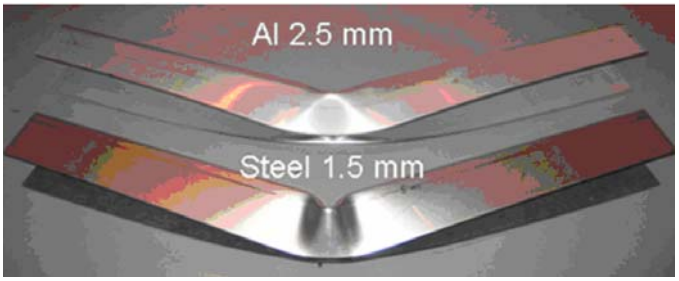

Figure 3: U-section collapse mode typical for all impact velocities

As beam deflection increases during loading cycle, the side walls start to move inward at the centre of the beam, so reducing the moment of inertia (MOI) in the section at the beam centre. A hinge develops as deflection increases still further. The load carrying capacity of the beam reduces as plasticity develops across the depth of the beam at the hinge, and load is at a maximum before a reduction in MOI occurs. Local deformation at the four support contact points is barely visible on the edge of beam – almost a witness mark. Measurements suggest local edge compression is typically less than 0.2 mm displacement, and extending over an arc length of less than 5 mm, although a lateral bulge is just visible. There was no evidence of edge cracking induced by tensile strain in any of the specimens tested across all velocities.

Measured load oscillation

Increasing load oscillation measured from the tranducer accompanies a higher velocity tup impacts, hence quantitative load measurement is restricted to 5000 mm/s velocity, see upper left and right figure 4. A ringing frequency common to velocities 2,000 and 5,000 mm/s observed in the upper figure 4 is determined at around 1 kHz. The first natural frequency of a simply supported beam with overhang symmetry[4] is calculated at 1 kHz. At 2,000 mm/s a lower frequency of 200 Hz is observed. The lower frequency appears to be excided at the start of the acceleration phase to reach constant velocity, before contact between tup and specimen as shown by the transducer signal response, see lower figure 4.

The lower ringing frequency of 200Hz is most likely inertial induced rather than friction resistance between tup and fixture guides; observe decay in oscillation at time 50msecs (lower figure 4) following initial acceleration phase. The lowest natural frequency of longitudinal vibration of tup shaft modelled as a simple spring mass assembly is around 2 kHz; since the strain gauge bridge circuit is mounted on tup shaft it dictates the frequency response of load measurement transducer. The lowest natural frequency of tup shaft in flexure is around 500Hz. The transducer strain gauges mounted on the shaft however, are configured as a full bridge circuit to compensate for flexing of shaft. Currently the source of the lower ringing frequency of 200Hz has not been identified.

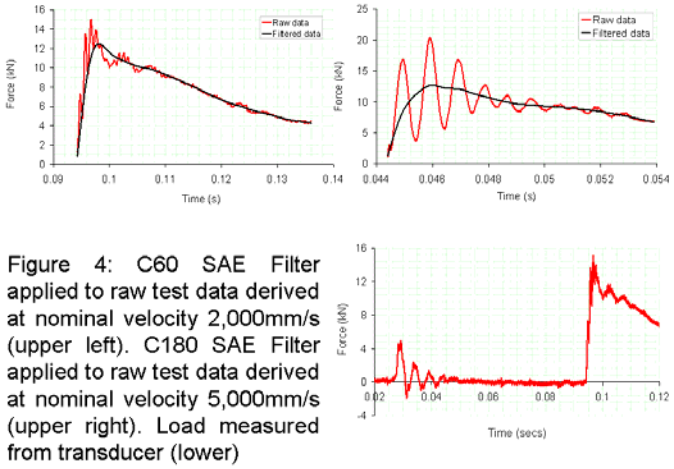

Figure 4: C60 SAE Filter applied to raw test data derived at nominal velocity 2,000mm/s (upper left). C180 SAE Filter applied to raw test data derived at nominal velocity 5,000mm/s (upper right). Load measured from transducer (lower)

EXPERIMENTAL RESULTS

The force versus displacement curves in upper figure 5 show velocity rate dependency. At the higher velocities of 2,000 and 5,000 mm/s initial stiffness (i.e. rate of change of force) reduces as force increases to its peak value resulting from use of filter. At 2,000 and 5,000 mm/s, the curve shape changes resulting from filtering the measured load oscillations, but a measurable dynamic effect is observed. Modeling investigations will confirm that the dynamic effect is in fact a measure of strength hardening resulting from the material strain rate effect. Although no quantitative performance data may be obtained above 5,000 mm/s, higher speed tests are useful in providing a qualitative measurement of material performance, specifically its ability to resist edge induced tensile fracture in the design range of interest.

Low speed test results are given for the aluminium alloy in the middle and lower figure 5. The middle figure shows the effect of sheet rolling direction for specimens which have undergone simulated heat treatment representative of paint bake process. The effect of heat treatment may be observed in the lower figure.

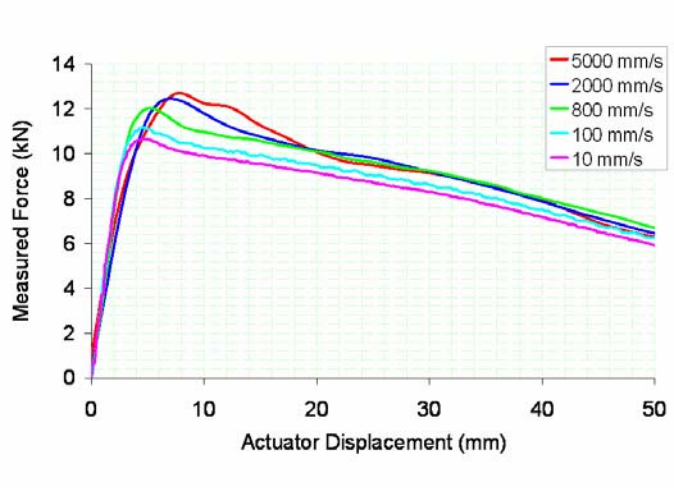

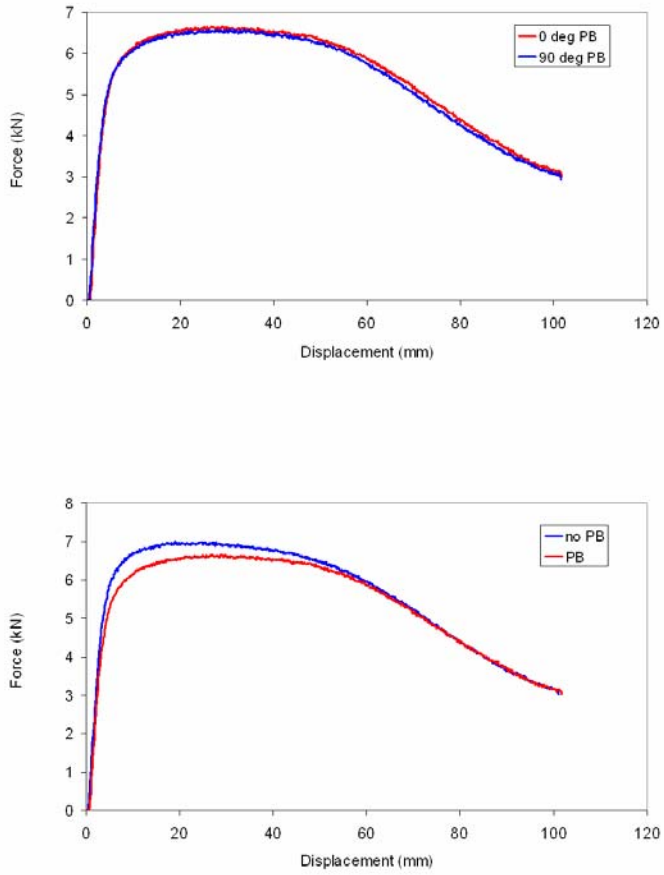

Figure 5: Speed rate dependency in steel specimens (upper). Effect of sheet rolling direction in aluminium alloy (middle). Effect of simulated paint bake on aluminium alloy (lower)

PERFORMANCE MEASURES

Performance measures to enable quantitative validation of material model with strain rate dependency are identified using the force-displacement curve. These are peak force and total energy at 50 mm displacement. A limit for the constant velocity boundary condition in the current fixture arrangement is 50 mm total displacement from initial tup contact with specimen.

MODELLING INVESTIGATIONS

The model of the experiment is shown in figure 7 below. The top of shaft is the machine actuator in which a constant velocity boundary condition is applied.

The shaft is modelled using solid elastic elements. Load measurement is modelled by simulating the strain gauge transducer on surface of shaft.

SPECIMEN GEOMETRY AND MESH DEFINITION

Mesh dependency to include element type, are investigated to establish the essential model input requirements to validate strain rate sensitive material model. The model of deformable specimen is developed using shell elements and the variations are shown in figure 8 for the dual phase steel specimen, and accompanying table. The nominal cross section dimensions width, depth and corner radius to mid-plane are common to all mesh variations however, mesh resolution obviously reduces in corner as element size is increased. For example, six elements are fitted to corner radius of geometry variant A, three elements to corner radius of geometry B, two elements to corner radius of variant C, two elements to corner radius of variant D, and one element to corner radius of variant E.

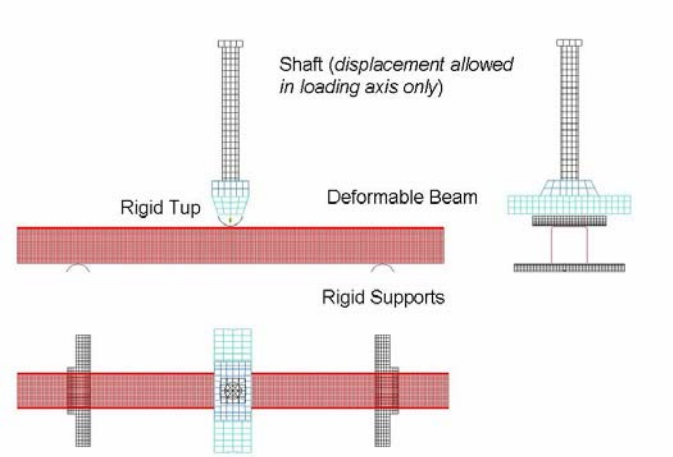

Figure 7: Model of experiment

Simulated experiments are conducted using a constant velocity boundary condition from quasi-static to 5,000 mm/s. For the quasi-static velocity boundary condition 800mm/s is applied using the quasi-static reference curve in the dynamic material model.

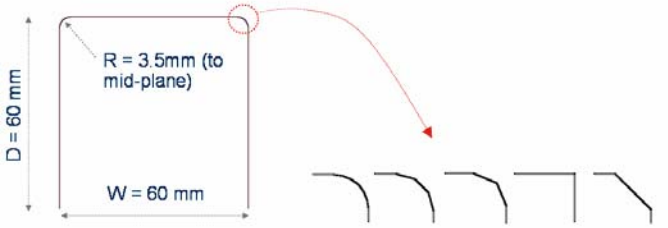

		A	B	C	D	E
Element Size (smallest dimension)	at Side and Top	2.5	5	5	5	5
	at Corner Radius	~1	~2	~2.5	~3.5	~5
No of Elements in Corner		6	3	2	2x90 deg	1x45 deg
Element Type		2, 16	2, 16	16	16	16
Constant velocity BC (mm/s) Applied		QS, 800, 2000, 5000	QS, 800, 2000, 5000	QS, 800, 2000, 5000	QS, 800, 2000, 5000	QS, 800, 2000, 5000

Figure 8: Model variations to be tested

MATERIAL MODEL

Strain rate dependent material tensile data and material model are developed following Ford Premium Automotive procedures[5] using IARC high speed precision servo-hydraulic test machine and model fitting routine. Raw high speed tensile data is generated across a spectrum of strain rates to create a set of material flow curves with strain rate dependency, see upper figure 9.

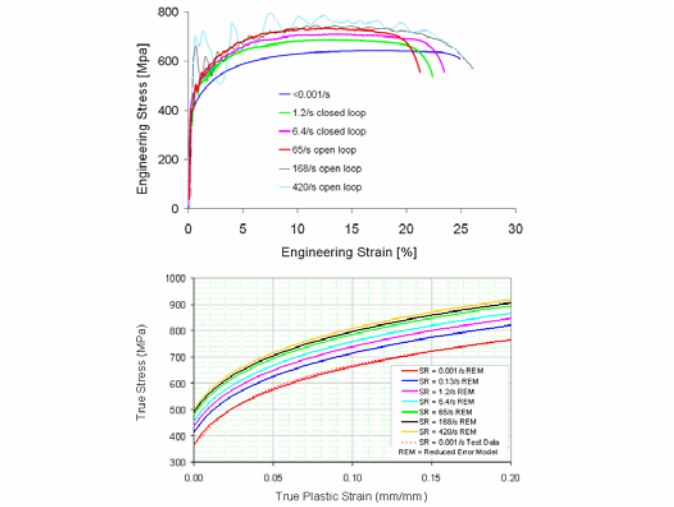

Figure 9: Raw strain rate tensile test results (upper). Fitted material model (lower)

The raw tensile data of upper figure 9 is pre-processed to create true plastic data for the region of uniform plastic elongation, and a surface model with two dependencies, stress as function of strain and strain rate, fitted to the raw plastic data to create a family of flow curves, see lower figure 9. Finally, the surface model is formatted using LS-DYNA MAT24[6] with table definition for strain rate dependency.

NUMERICAL CALIBRATION OF TRANSDUCER

The simulated strain gauges on the transducer are calibrated at low speed using the either spring or contact force output from model. Model correlation to low speed test result for Dual Phase steel using the refined mesh variant A and element type 16 is shown in figure 10 below, and demonstrates a good fit to the experimental result.

DYNAMIC EFFECT ON MATERIAL PROPERTY MEASUREMENTS

The dynamic effect on material strain rate sensitivity measurements is studied using model. The model of specimen uses refined mesh variant A and element type 16. The quasi-static material curve in the dynamic material model of figure 9 is the material input to model of specimen to study dynamic effect.

Constant velocity boundary conditions 800, 2,000 and 15,000 mm/s are applied to the tup in turn. High measured load oscillation is observed at 15,000 mm/s as shown in the upper figure 11. Comparing filtered results at different velocities, peak force is broadly consistent for increasing velocity, unlike displacement to peak force, which is due to use of filter. It is confirmed that force measurement is restricted to 5,000 mm/s velocity for the current test arrangement.

The frequency response of the load measurement is computed at velocities 2,000, 5,000 and 10,000 mm/s, and the result is shown in lower figure 11. The dominating frequencies are determined at 1 and 2 kHz; respectively these correlate to natural frequency of specimen and frequency response of load measurement transducer in longitudinal vibration.

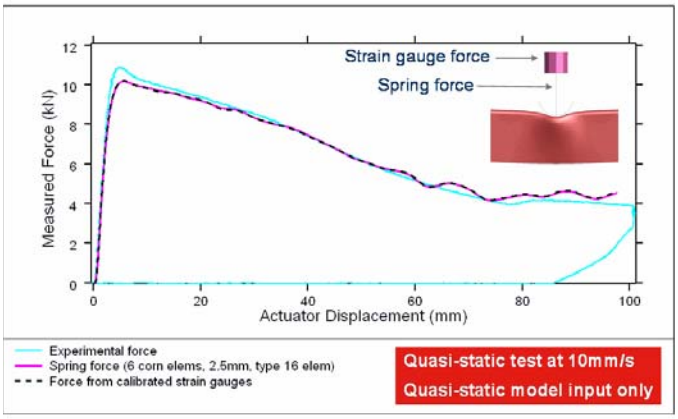

Figure 10: Calibration of simulated force transducer

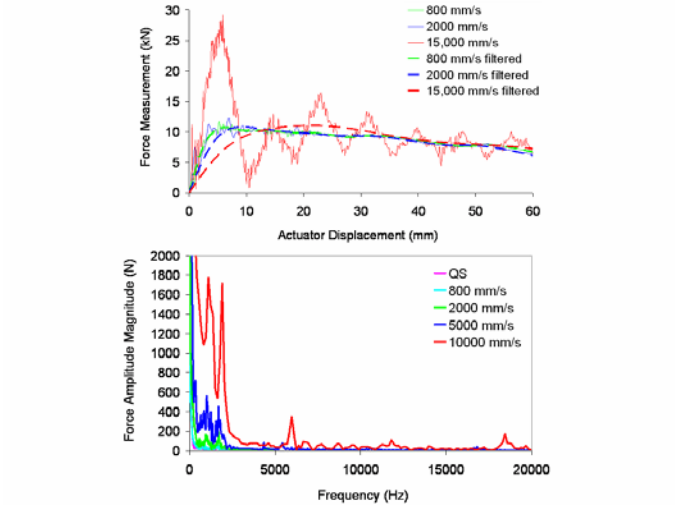

Figure 11: Modelling dynamic effect using quasi-static material curve (upper). Load oscillation frequency response (lower)

MODEL RESULTS

The solver LS-DYNA 970 6763 SMP and 4-way IBM set at double precision was used in computations, and OASYS[7] Pre and Post-processing to support analyses. The deformed shape of model beam is consistent with the experiment, as shown in figure 12 for all model mesh and velocity variants.

Figure 12: Typical response of deformable structure

EFFECT OF MESH REFINEMENT

Some of the results of model calculations for the variations described in figure 8 are shown in figure 13 below.

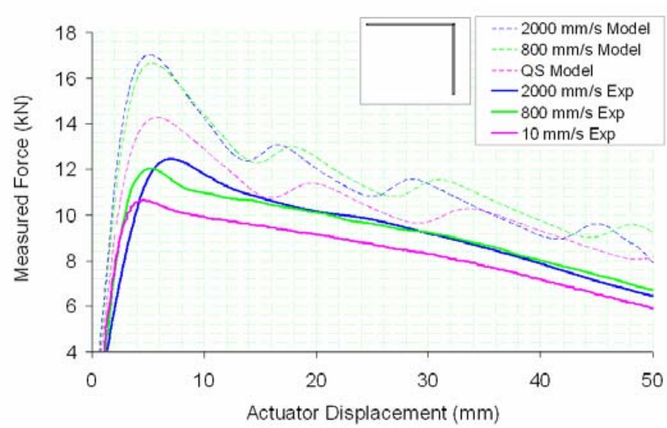

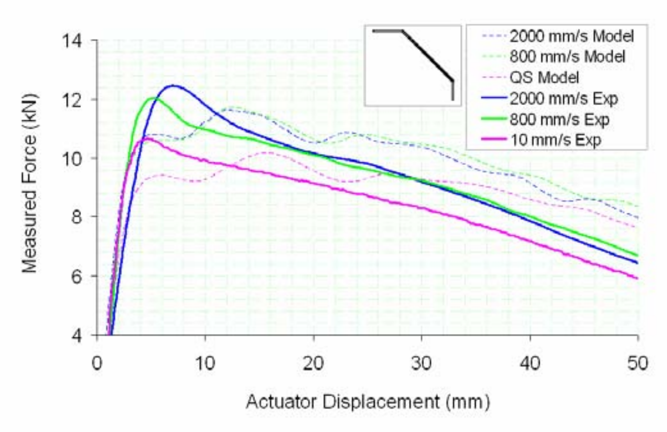

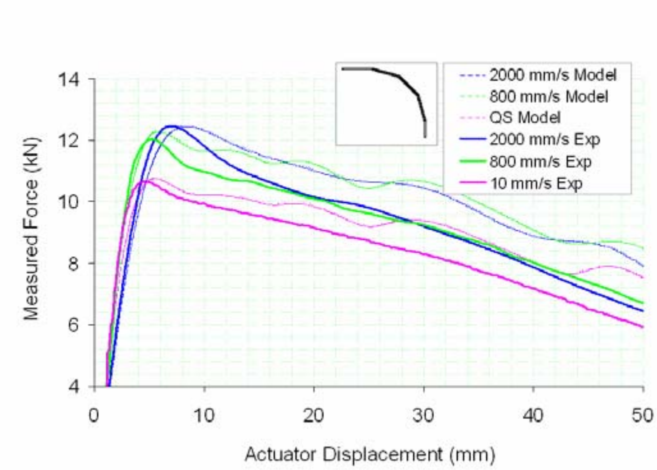

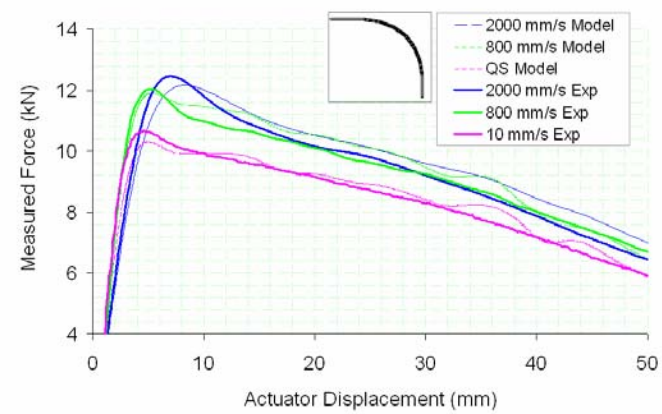

Figure 13: Upper model result is variant D and element type 16. Second model result down is variant E and element type 16. Third model result down is variant B and type element 16. Lower model result is variant type A and element type 16.

DISCUSSION OF RESULTS

For the two performance measures, all results are summarised in the two bar graphs of figure 14.

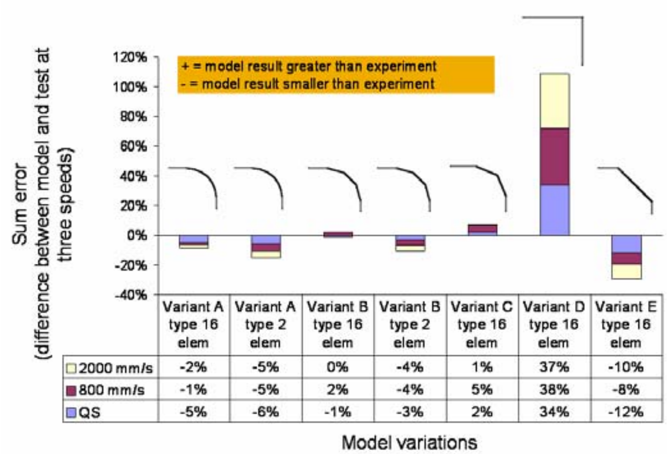

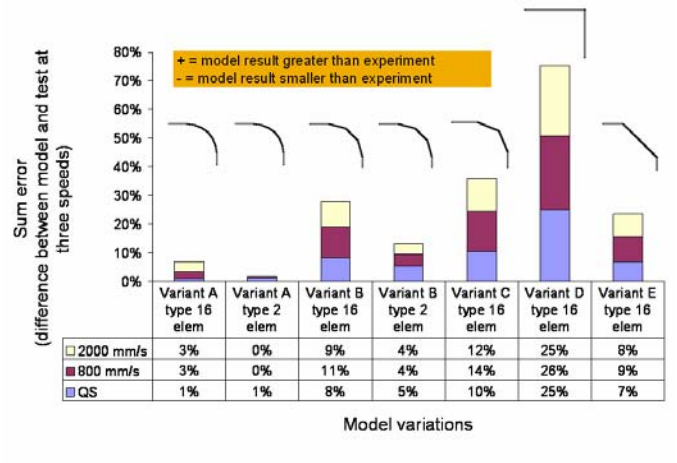

Figure 14: Upper bar graph compares difference in peak force between model and test result. Lower graph compares difference in total energy (at 50mm displacement) between model and test result.

Difference in peak force between model and test result

The colour in the bar graph identifies the speed at which the difference is computed. So we may observe the error is roughly equal at each speed.

In the upper graph of figure 14, a large difference between model and test result is observed for 2 x 90 degree corner elements (variant D) and also for 1 x 45 degree corner element (variant E). Positive error implies the model result is stiffer than the test result. Conversely, a negative error implies the model is less stiff than the test result.

The model results using element type 16 for mesh variants A, B and C delivered the lowest error at below 5%. Variant C delivered a slightly over stiff result.

All model results using element type 2 for variant A and B are under stiff of the order 5% for each speed tested. It is also noted that type 2 elements in LS DYNA appeared to hourglass readily even with the appropriate settings in the hourglass control card activated.

Difference in total energy (at 50 mm displacement) between model and test result

In the lower graph of figure 14, the result giving the lowest error is variant A. This model uses element type 16, with 6 corner elements and mesh density comprising 2.5 mm square shells over the top and sides of channel.

APPROXIMATE CALCULATION OF PEAK STRAIN RATE IN SPECIMEN

Model stress contours in the Dual Phase sheet steel specimen are shown in figure 15 for low speed loading. The fringe contours show tensile and compressive deformation in the lower and upper section of beam either side of the neutral axis at small displacement. The peak strain rate at the centre of beam channel may be approximated by the simple formula shown in upper figure 15 for small displacement. At 5 m/s peak strain rate may reach approximately $20s^{-1}$ when subjected to 5 m/s tup impact speed.

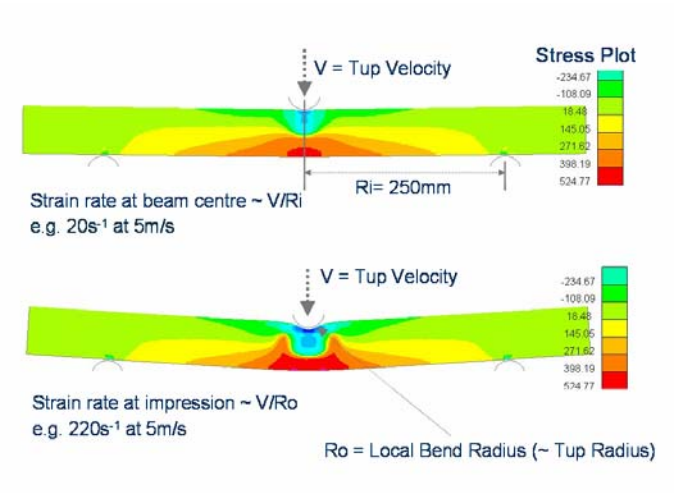

Figure 15: Model stress contours in Dual Phase sheet steel open channel beam subjected to 3-point bend

At higher displacement as shown in lower figure 15, and as the hinge starts to develop, the peak strain rate in the depression made by the tup may be approximated at $220s^{-1}$ for a tup impact speed of 5m/s and tup radius used.

CORRELATION BETWEEN ALUMINIUM MODEL AND TEST RESULT

Using the refined mesh of model variant A, the goodness of model fit to experimental results for a work hardening grade aluminium alloy (AA5000 series) is demonstrated in figure 16 for low speed loading.

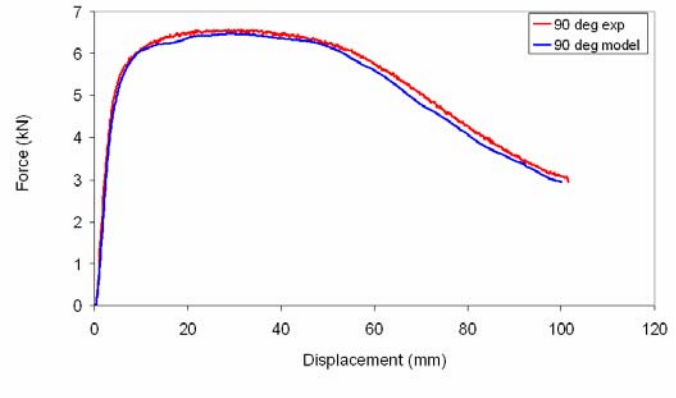

Figure 16: Aluminium alloy model correlation

The capability of the test procedure to support the validation of material data with strain hardening resulting form either fabrication or forming is shown in figure 17. A thermally activated recovery process develops in the material during the simulated paint bake process. The

result is a reduction in the level of work induced strain hardening which developed in the corners of the specimen from the fabrication process. The material tensile data input to model of specimen is in the as-received condition; this is the result shown in figure 16 and is also given in the lower curve of figure 17.

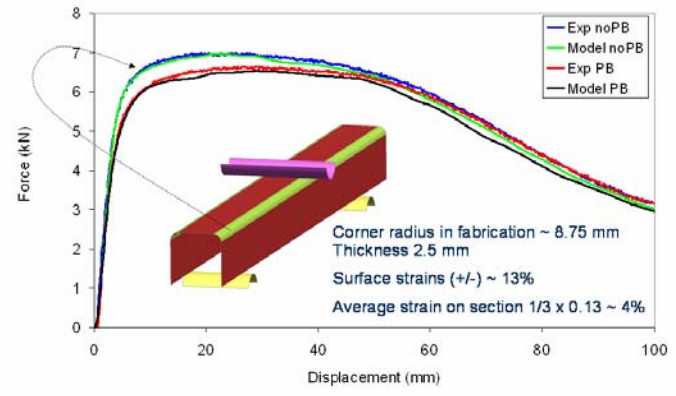

Figure 17: Aluminium alloy model correlation using strain hardened properties

The upper curve in figure 17 is the result of the specimen that had not received a simulated thermal paint bake treatment. The response is stiffer due to the strain hardening in the corners of the specimen. This is confirmed by the model, in which representative strain hardened properties of the material are input to corner of specimen, and demonstrates good agreement with experimental results. The material input to corners of model assume isotropic material hardening and this was generated by simply offsetting the strain axis (~ average 4% across section) in the material card by the equivalent forming strain.

EFFECT OF DELAYED DEVELOPMENT OF PLASTIC HINGE IN ALUMINIUM ALLOY

The ability of the aluminium alloy to resist formation of a plastic hinge is improved over the steel because the gauge is thicker, and local buckling of section is delayed e.g. inward movement of side walls of channel at centre of section. This is evidenced by the results in the graphs in figure 5. The force measured in the steel specimen is initially higher but it also exhibits a higher rate of load decay compared to the aluminium alloy.

The consequence is that the aluminium alloy sustains higher tensile strain in side walls of beam channel as shown in figure 18. Since ductility is generally expected to reduce in higher strength materials, such materials may be more prone to edge induced tensile fracture. Note also that press-stretch forming strain will also reduce ductility. Such effects can be checked using the bend-impact test procedure described in this paper for the crash speed range of interest.

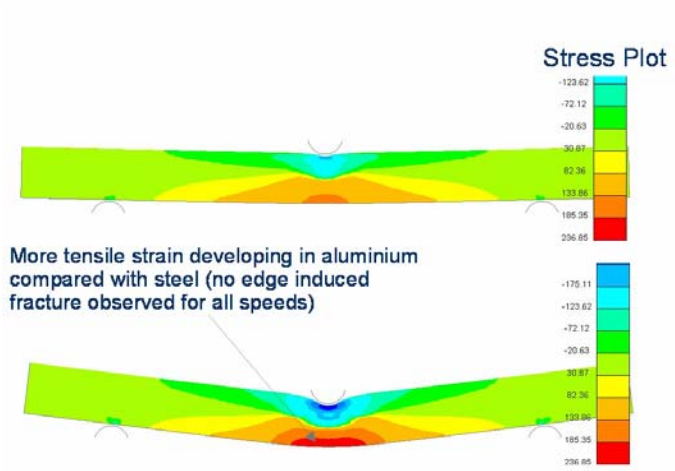

Figure 18: Model stress contours in aluminium alloy sheet open channel beam subjected to 3-point bend

CONCLUDING SUMMARY

The test procedure is capable of generating meaningful quantitative measurements in the velocity range 10 mm/s through to 5,000 mm/s. Measurements from test include force, time and displacement, from which the developed velocity may be derived during loading cycle. Under open loop control (velocity above 1,000 mm/s), average relative deviation from the target velocity is measured at -7%. The measured velocity is however repeatable for the same test conditions, hence if necessary velocity profile correction may be used to compensate velocity reduction by tuning flow through machine hydraulic valves, and reduce measured deviation from target velocity. Under closed loop control (velocity below 1,000 mm/s) the average relative deviation from target velocity is measured at +3%.

Although no quantitative performance data may be obtained above 5,000 mm/s, the test is useful in providing a qualitative measurement of material performance, specifically its ability to resist edge induced tensile fracture in the design range of interest for crash structures. For the material tested, edge cracking was not visible in the material; note the open channel beam was fabricated by folding hence the developed forming strains are restricted to the corners. It is important to test a materials resistance to fracture using a beam channel with modest thinning strain in side walls resulting from press-stretch forming.

Modelling and experiments have shown a measurable strength hardening effect in the steel material in the velocity range 10 to 5,000 mm/s, which is attributed to material strain rate sensitivity.

The goodness of model fit to experimental results is dependent on mesh resolution on sides and faces of channel, refinement at corner and element type. The level of refinement to validate material strain rate sensitivity data for use in crash simulation tools has been established using a Dual Phase steel. The level of

mesh refinement was demonstrated also by the fit of aluminum model to test results; showing sufficient sensitivity to discern the influence of forming strain in the corner of fabrication.

Using the performance measures peak force and total energy at 50 mm displacement, the best model fit is variant A with type 16 element; this mesh uses a 2.5 mm element size and 6 corner elements (~ 1 mm); the error is in the order of a few percent. Although element type 2 together with 5 mm element size and 3 corner elements (~ 2 mm) gives a similar level of error, type 2 elements are prone to hourglassing and this will affect local model property measurements such as strain and strain rate. In general increasing element size delivered an increasingly stiffer response. Of note are model variants D and E, respectively one corner element at 45 degree and two corner elements (each roughly 3.5 mm) at 90 degree. The 45 degree corner element is a poor fit to the experimental result, giving an error in the order ten percent for two performance measures considered. The 90 degree corner element is a very poor fit, giving an error in the order tens of percent.

MODELLING RECOMMENDATIONS

To validate material data with strain rate and forming strain dependencies, a high level of mesh refinement in model is recommended, typically 2.5 mm shell element size and a minimum of 3 corner elements, together with use of element type 16. For industrial modelling applications, a 5 mm shell element size is recommended together with minimum of 2 corner elements and element type 16 to model automotive crash structures.

ACKNOWLEDGMENTS

To thank the industrial partners CORUS, NOVELIS, ARUP, MIRA, DUTTON SIMULATION, RICARDO, ARRK, GOM UK and HBM in addition to those named authors and companies, for supporting and engaging in this collaborative research project.

REFERENCES

1.http://www.worldautosteel.org/pdf_hsrt/RptRndRobResults.pdf
2. BS EN 10002-1:2001 (low speed tensile testing of metallic materials and mechanical property characterisation)
3. VHS 160/100-20 High Strain Rate Test System and Accessories, Instron Ltd, Coronation Rd, High Wycombe, Bucks, England
4. Murphy J. F. “Transverse Vibration of a Simply Supported Beam with Symmetric Overhang of Arbitrary Length,” Journal of Testing and Evaluation, JTEVA, Vol.25, No. 5, September 1997, pp. 522-524
5. P.K.C.Wood et. al., “An Improved Test Procedure for Measurement of Dynamic Tensile Mechanical Properties of Automotive Sheet Steels,” SAE International 2007-01-0987, Detroit, April 2007.
6. Hallquist, J. O., LS-DYNA. Keyword User’s Manual. Version 971, Livermore Software Technology Corporation, Livermore, 2007.
7. OASYS LS-DYNA ENVIRONMENT, The Arup Campus, Blythe Valley Park,
Solihull, West Midlands, B90 8AE

CONTACT

Dr Paul Wood is Project Manager for Materials Technology to support Premium Automotive Product Development at the IARC. Customer enquiries are welcomed. Email: p.k.c.wood@warwick.ac.uk / UK 0044 (0) 7932 608084

DEFINITIONS, ACRONYMS, ABBREVIATIONS

IARC: International Automotive Research Centre

Relative error: (actual value-correct value)/correct value